*Proceedings of the 8th **ICCAE-8** Conference, 25-27 May, 2010*

Military Technical College
Kobry El-Kobbah,
Cairo, Egypt

8th International Conference on Civil and Architecture Engineering
ICCAE-8-2010

A Low-Cost Photogrammetric System for Structural Deformation Monitoring

By

Ivan Detchev   Ayman Habib*

Abstract:

As a remote sensing technique, photogrammetry does not need access to objects being measured. This can be a great advantage when it comes to deformation monitoring. This paper proposes a low-cost photogrammetric system for deformation monitoring of structural materials. The system design is based on a setup consisting of a projector and multiple cameras, and it is using a pattern projection. The software necessary to perform the 3D object reconstruction includes modules dealing with epipolar resampling, feature extraction, matching and tracking, and 3D multiple light ray intersection. The system was tested by first fitting a point cloud reconstruction of a flat particle board to a mathematical plane. Then, the same particle board was artificially deformed, and the normal distances from the new point cloud reconstruction to the original fitted plane were calculated. The experiment proved that it was possible to detect sub-millimetre level deflections.

Keywords:

Close range photogrammetry, off-the-shelf digital cameras, electronic projectors, pattern projection, 3D object reconstruction

---

* Department of Geomatics Engineering, University of Calgary, Canada

1. Introduction:

Deformation monitoring techniques can be divided into geotechnical measurements and geomatics-based surveys. The geotechnical measurements are made with extensometers, tiltmeters, micrometers, etc., which yield the magnitude of the deformation relative to reference marks on the actual object being monitored. On the other hand, geomatics-based surveys include traditional terrestrial surveying with precision levels, theodolites and electronic distance measurement devices, global navigation satellite system positioning with geodetic grade receivers and antennas, and remote sensing techniques including photogrammetry. The advantage of the geomatics-based surveys for deformation monitoring is that the instruments used allow for the determining of the deformation on an absolute scale, i.e. the points measured on the object of interest are tied to other points belonging to a reference coordinate frame. Moreover, these methods allow for redundant measurements whose precision can be evaluated by a least squares adjustment [1].

The remote sensing techniques of doing precise measurements have an even further advantage – there is no need to access the object being monitored. For example, photogrammetry (i.e. the reverse process of photography) uses multiple 2D images of a 3D object taken from different locations to reconstruct that object as a digital model. The classic scenario in photogrammetric reconstruction is the stereo photography case (see ***Figure 1***), where conjugate points are identified in the left and right images, and together with the knowledge of the location of the left and right camera perspectives centres, and the orientation of the left and right light rays, the location of the point of interest is intersected in the object space. The mathematical model used for 3D object point reconstruction is the collinearity equations [2]:

$$
\begin{aligned}
x &= x_P - c \cdot \frac{r_{11} \cdot (X - X_0) + r_{21} \cdot (Y - Y_0) + r_{31} \cdot (Z - Z_0)}{r_{13} \cdot (X - X_0) + r_{23} \cdot (Y - Y_0) + r_{33} \cdot (Z - Z_0)} + \Delta x \\
y &= y_P - c \cdot \frac{r_{12} \cdot (X - X_0) + r_{22} \cdot (Y - Y_0) + r_{32} \cdot (Z - Z_0)}{r_{13} \cdot (X - X_0) + r_{23} \cdot (Y - Y_0) + r_{33} \cdot (Z - Z_0)} + \Delta y
\end{aligned}
\tag{1}
$$

Other than not having to directly access the object being monitored, remote sensing techniques can be automated. This can reduce the effects of any human errors due to performing tedious tasks during repetitious inspections. For example, the de la Concorde overpass in Laval, Quebec, collapsed a few hours after a structural inspection, which revealed no anomalies. In addition, current photogrammetric reconstruction systems can be built from inexpensive and replaceable sensors, which are two of the desired criteria of current structural monitoring systems [3]. This is because low-cost and off-the-shelf digital cameras and short throw digital projectors are now flooding the market for electronic products, and they are replacing the expensive metric cameras and custom made analogue projectors used in close-range photogrammetry. The use of such digital cameras and projectors is becoming a convenient and an inexpensive alternative for 3D reconstruction applications such as cultural heritage documentation, facial reconstruction, biomedical imaging, and also – structural deformation monitoring. This study is thus motivated to investigate the potential for deformation monitoring of structural materials using a photogrammetric system, which performs 3D reconstruction based on multiple digital cameras and projectors. The next two sections will describe the proposed system design and the methodology for the surface model generation, which will be followed by experimental results and conclusions.

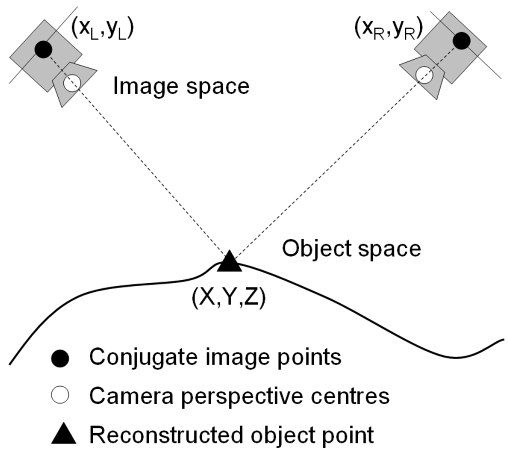

Figure 1: *Stereo photography for object space reconstruction*

<u>**2.Proposed System Design:**</u>

The proposed system design addresses the set of objectives listed as follows. First, the system has to be built from low-cost and off-the-shelf components. Second, the system should have millimetre level of accuracy so that it can be used for deformation monitoring applications. Lastly, the data processing for the system should be automated, it should not require high level of expertise for the user, and the final product should be delivered quickly to the client.

So in the proposed photogrammetric system, several low-cost off-the-shelf digital cameras and an accompanying digital projector are fixed on a metal arm. This constitutes one scan arm (see ***Figure 2a***). All cameras are synchronized to operate simultaneously thus producing a surface model of the object placed in front of the scan arm (see ***Figure 2b***). The next subsections deal with the necessity for a system calibration, the use of a pattern projection, and the justification for having multiple cameras in a scan arm.

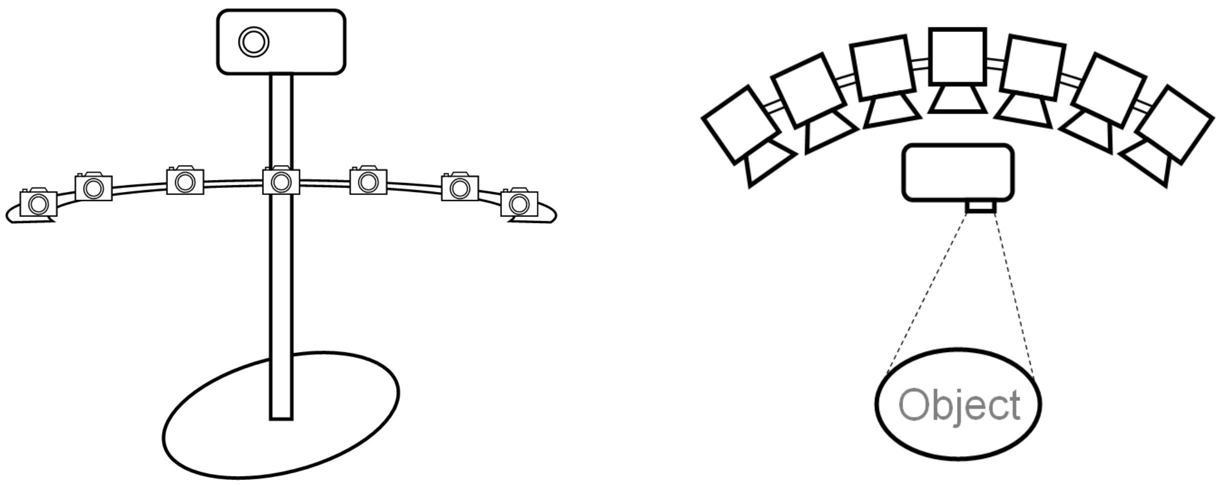

(a) (b)

Figure 2: *Front (a) and top(b) views of the proposed system*

System Calibration: The employed cameras must be calibrated before use. The objective of the calibration process is to obtain the camera's internal characteristics or interior orientation parameters (IOPs), which include the principal point coordinates, the principal distance, and the lens distortion parameters [4]. The cameras should also undergo a stability analysis procedure, which verifies that the estimated IOPs do not change significantly over time. The stability analysis procedure is necessary, because the cameras used are off-the-shelf ones and they were not designed specifically for metric applications [5]. The location and orientation, i.e. the exterior orientation parameters (EOPs), of each camera station are obtained through a bundle adjustment procedure using a test field with pre-surveyed target points. Since the cameras are rigidly mounted on a metal arm, their relative EOPs should stay the same for each scan arm. Thus, the bundle adjustment for each scan arm is required to be done only once.

Pattern Projection: The purpose of having a projector in the proposed photogrammetric system is to project a pattern (see ***Figure 3***) onto the object of interest in order to provide artificial markers on its surface. This is necessary, because often times object surfaces are relatively homogeneous and with no artificial markers it would be impossible to identify conjugate points in the captured stereo pairs (see ***Figure 4***). Also, by regulating the resolution of the projected pattern, the density of the final generated point cloud can be controlled. The projected pattern is generated by randomly arranging eleven unique 3x3 pixel sub-blocks. However, to minimize any matching ambiguity, no sub-block is repeated within a radius of six pixels. During the projection of the pattern, the lighting must be managed so that optimal contrast of the artificial features is achieved on the surface of the subject of interest.

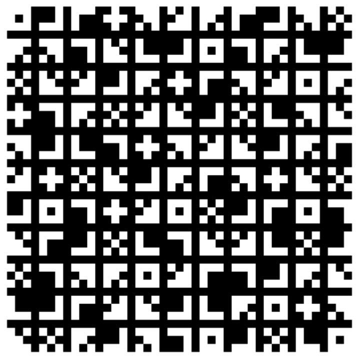

Figure 3: *Designed pattern for projection*

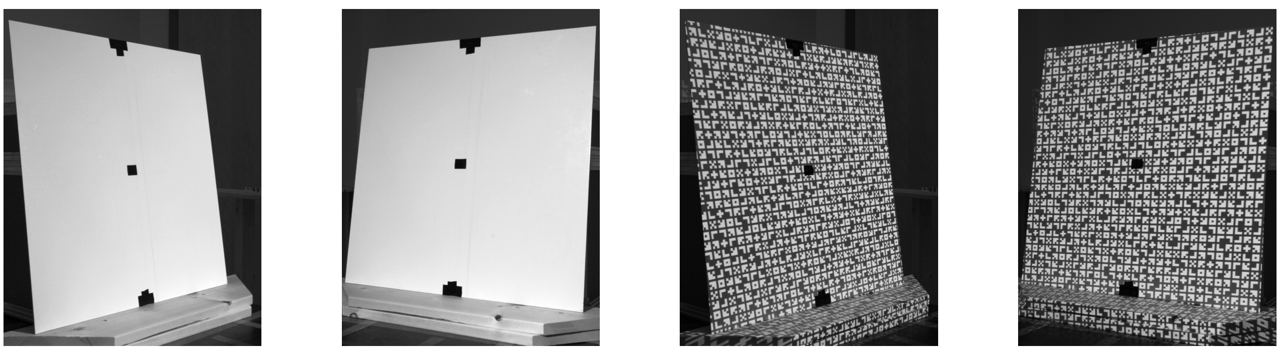

(a) (b) (c) (d)

Figure 4: *Example of a flat metal plate imaged without (a, b) and with (c, d) a projected pattern*

Balance between Intersection Accuracy and Matching Reliability: In order to solve for the 3D object space coordinates of points on the surface of the object, these points must be first identified in the image space. The identification of conjugate points in overlapping images is preferably done through an automated matching procedure in order to speed up the processing time and also to minimize the level of expertise required. In automatic image matching, conjugate points are identified through a measure that quantifies the degree of similarity between regions in the overlapping areas of the images. The closer two camera stations are positioned, the less impact from relief displacement there is. This leads to higher similarity between the captured images, and the automated matching procedure becomes more reliable. This is why a short baseline between two camera stations is ideal when it comes to automated image matching. On the other hand, the baseline between two camera stations in traditional stereo photogrammetry must be sufficiently large so that the intersection angle of two conjugate light rays is as close to 90° as possible. This large baseline camera station geometry optimizes the intersection accuracy, but it usually causes significant relief displacement between the images, and the automated image matching becomes problematic [6]. This is why, in the proposed system, the object of interest is simultaneously photographed using multiple cameras from different viewpoints which are close together, and automatic image matching is performed between the adjacent exposure stations with short baselines. After that, conjugate points are tracked through all the images, and every point is reconstructed through conjugate light ray intersection from multiple images. In this manner, the procedure generates a surface model by taking advantage of the reliable matching in the images with short baselines and the accurate multiple light ray intersection from the images with large baselines.

3.Surface Reconstruction:

The image data is first collected with the multiple cameras from the above described system, and then it is processed for the generation of the 3D surface model of the object of interest. This is achieved by carrying out corner detection on every image, doing image matching for every stereo pair in order to identify conjugate corner points, tracking the same matched corners through the neighbouring stereo pairs, and finally intersecting the multiple light rays coming from the tracked corners. These procedures are described in the following two subsections.

Corner Detection and Image Matching: In order to optimize the total processing time, the corner detection and the image matching are restricted to a region of interest, i.e. the region occupied by the object being mapped, and the image space outside of this region is ignored. The region of interest is manually defined by the user in terms of a binary mask (see ***Figure 5***). The rest of the surface reconstruction processing is fully automated.

The next step in the surface reconstruction processing is identifying features of interest in every image. In the case of the proposed system, the features of interest are the corners in the projected pattern, and they are extracted using the Harris operator [7]. Further on, the image matching algorithm of choice for the system is based on normalized cross correlation (NCC), which is an efficient technique for performing area-based matching [8]. In addition, in order to decrease computational time and to avoid matching ambiguity, the matching space is reduced by two constraints. First, the y-parallax is eliminated in order to constrain the matching space in the row direction, and second, the x-parallax is predicted in order to constrain the matching space in the column direction. The former is accomplished by performing epipolar resampling (see ***Figure 6***), and the latter by employing a hierarchical matching strategy [9].

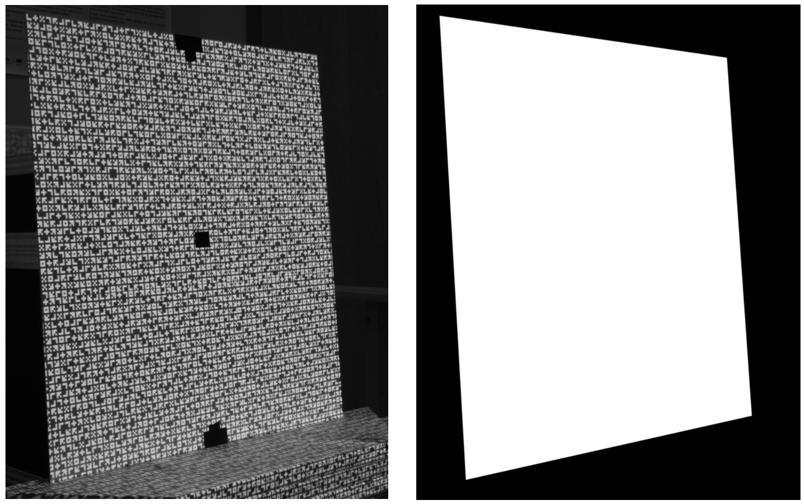

(a) (b)

Figure 5: *Example of an original image of a flat metal plate (a), and a region of interest mask (b)*

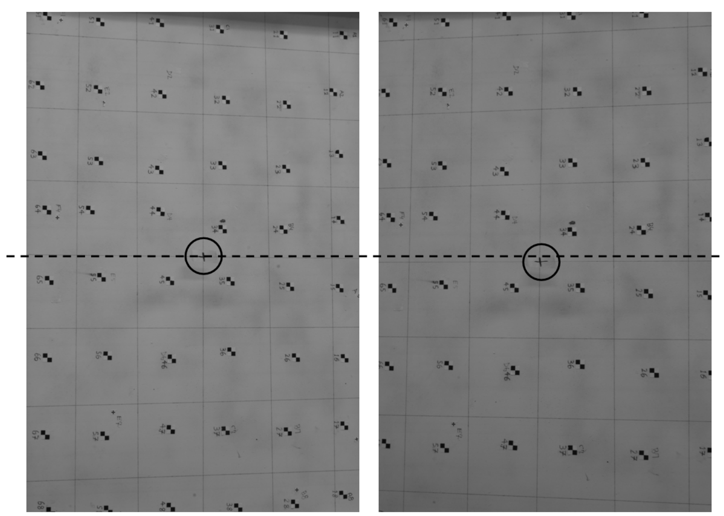

(a)

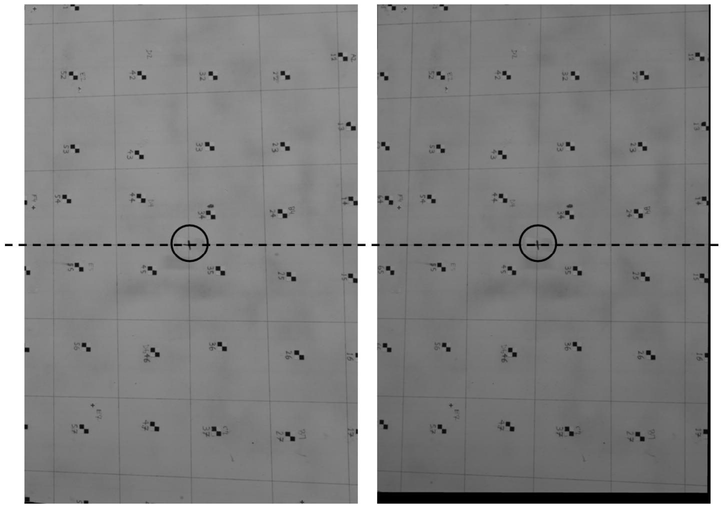

(b)

Figure 6: *Conjugate points appear on different rows in the original stereopair images (a), and on the same image row after normalization according to epipolar geometry (b)*

Tracking and Intersection: After the image matching is performed, corner tracking is done to identify the same corners in all the images they appear in. Effectively, the tracking procedure yields the image coordinates of conjugate corners, which are needed for the multiple light ray intersection. Along with the IOPs of the involved cameras, and the EOPs of the involved images, these image coordinates are included in a least squares adjustment to determine the object coordinates of the corresponding points on the surface of the object being reconstructed. ***Figure 7*** shows examples of the reconstruction results.

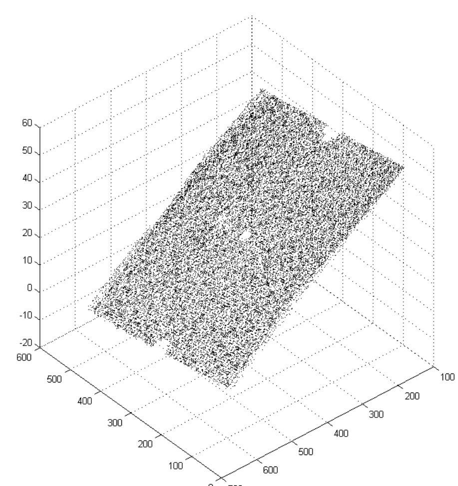

Figure 7: *Example of a reconstructed flat metal plate*

The multiple light ray intersection completes the data processing steps. The order of the necessary procedures is summarized in ***Figure 8***.

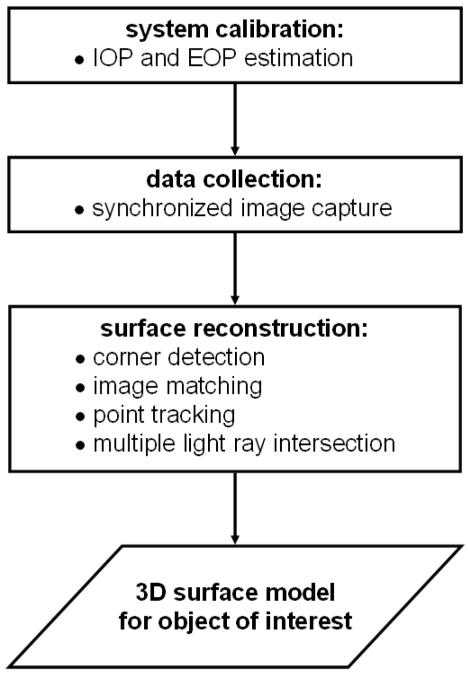

Figure 8: *Proposed procedures for 3D surface reconstruction*

4. Experimental Results:

There were two experiments carried out for this paper. The objectives of these experiments were to test the feasibility and estimate the accuracy of the proposed system, i.e. to verify that the system was fit to perform reconstructions for industrial quality control and infrastructure monitoring (e.g. beams under different loading conditions). The images required for the surface reconstruction were captured with seven digital single-lens reflex (DSLR) cameras. Each camera had a 22.2mm x 14.8mm complementary metal oxide semiconductor (CMOS) solid state sensor. The output images had 3888 rows and 2592 columns or 10.1 effective megapixels, where the pixel size was 5.7μm. The lenses of the cameras had a nominal focal length of 35mm. The seven DSLRs were rigidly mounted to a wooden frame representing the scan arm in the proposed system design. The camera positions were evenly spaced, and the baseline distance between neighbouring exposure stations was approximately 0.4m. In addition, the cameras were accompanied by a single-chip digital light processing (DLP) short throw projector, which had an extended graphics array (XGA) with a resolution of 1024 pixels x 768 pixels. A flat particle board with dimensions 60cm x 60cm, and thickness of 0.5cm was placed 1.1m away from the exposure stations on the constructed scan arm. The seven cameras were synchronized with a remote control, and the images for each of them were taken simultaneously.

The first experiment was to reconstruct a 45cm x 45cm portion of the flat particle board. The total number of reconstructed points was 22,350. This amounted to an average point density in the order of 10 points/cm^2. A mathematical model for a plane was fitted to the data set. The average normal distance was zero millimetres, and the standard deviation was ±0.39mm. The minimum and maximum signed normal distances were -2.6mm, and +2.3mm, respectively. The execution for the reconstruction of the board surface model took over three hours. The bulk of the processing time, i.e. 30 minutes per stereo pair on average, was spent for the hierarchical image matching.

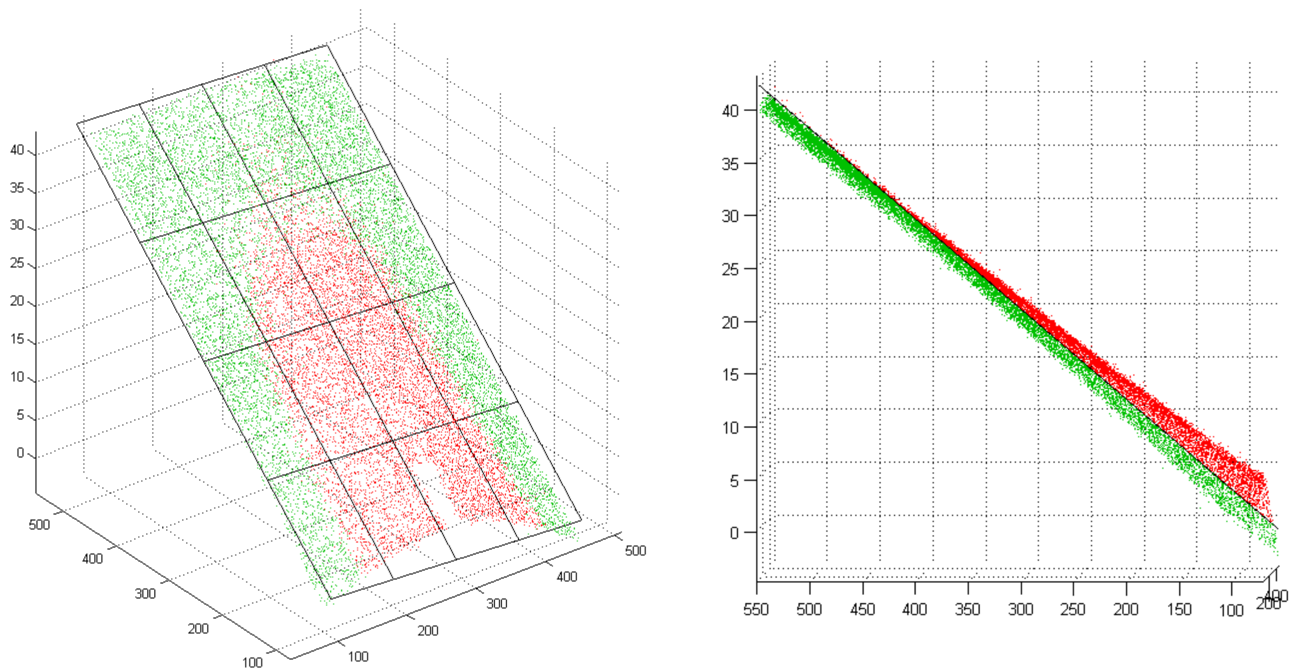

(a) (b)

Figure 9: *3D (a) and side (b) view of the board deformation: the solid grid represents the plane defined by the reconstructed points from the first experiment, and the red (above the plane) and green (below the plane) points represent the deformed board from the second experiment (units are in mm)*

During the second experiment a 40cm x 40cm portion of the same particle board was reconstructed, however, this time the board was artificially bent in order to simulate a structural deformation. The bending was done at the same place where the board was imaged for the first experiment, i.e. other than the board deformation there was no other translation or rotation present in the setup. This was achieved by securing the particle board to a solid baseboard with several crews (0.2mm in diameter and 10cm in length), and two heavy duty clamps. The 17,665 reconstructed points from the second experiment were fitted to the mathematical plane defined by the points from the first experiment (see ***Figure 9***). The average normal distance was again zero millimetres, but the standard deviation this time was ±1.19mm. The range of the signed normal distances also increased – the minimum and maximum values were -4.1mm and +4.3mm, respectively (see ***Figure 10*** and ***Figure 11***).

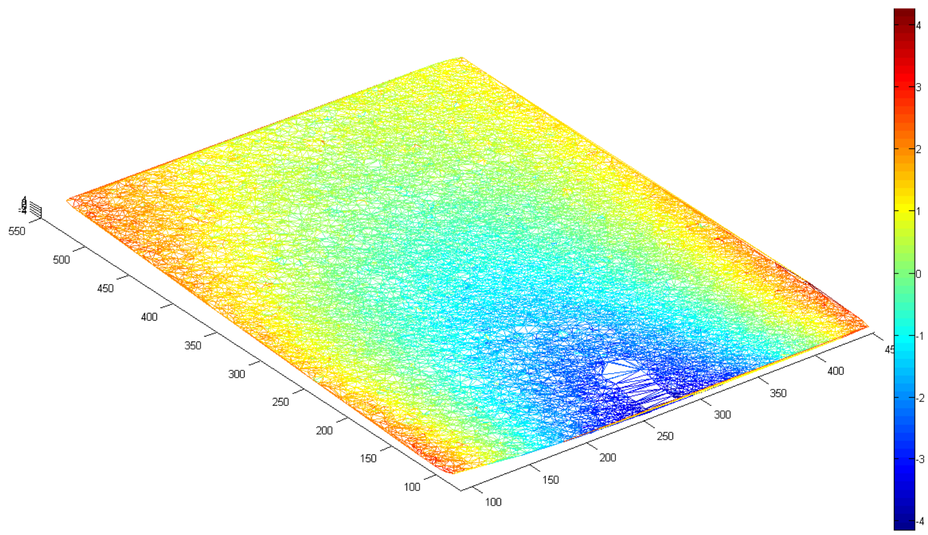

Figure 10: *Range of normal distances (units are in mm)*

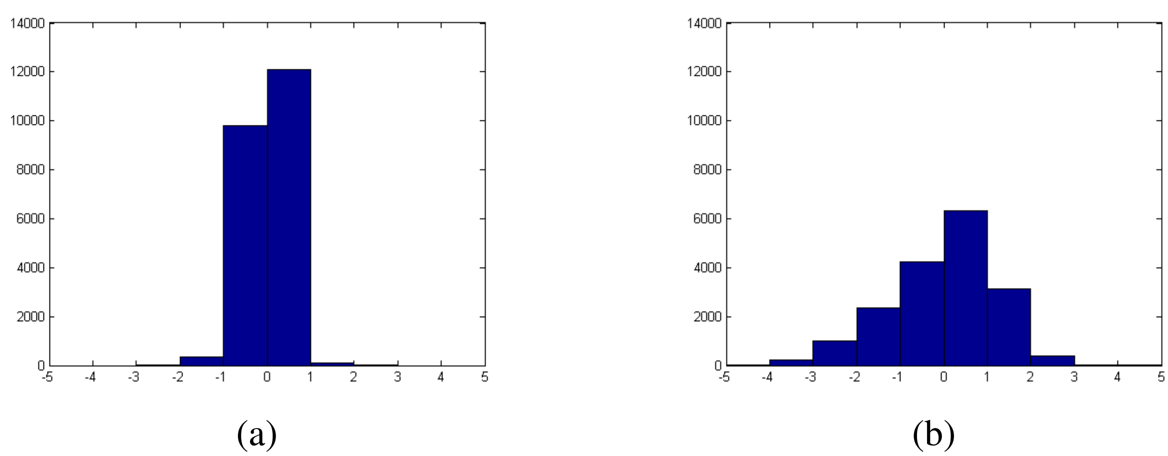

Figure 11: *Histograms of the signed normal distances from experiment 1 (a), and experiment 2 (b) (x-axis units are in mm)*

5. Conclusions and Recommendations for Future Work:

This paper suggests the use of a photogrammetric system for 3D object reconstruction in order to perform deformation monitoring. The proposed system is based on a low-cost multiple-camera setup and a pattern projection, and it was built by only using off-the-shelf components. The processing procedures include semi-automated surface reconstruction, where the only manual involvement in the surface reconstruction is selecting a region of interest for the corner detection and matching. The performance of the implemented proposed system was assessed by fitting a mathematical plane to the reconstructions of a flat and a deformed particle board. The final reconstructed models exhibited sub-millimetre precision, which was enough to detect a deflection on the millimetre level. Since the experimental results were encouraging, the proposed system is thought to be sufficiently accurate for applications involving deformation monitoring of structure materials. All in all, the implemented system met all original objectives, except that processing the data takes longer than required. Thus, current work is focusing on increasing the automation and speeding up the time required for processing. Future work will involve building an actual metal frame for the cameras and also including the projector not only for projecting the pattern, but also as part of the reconstruction processing. The system will also be tested outside the lab, i.e. in the field, at usual operational conditions.

Acknowledgements:

The authors would like to thank the NSERC Strategic Grant program for partially funding this research project.

Nomenclatures:

(x, y) …	Observed image coordinates
(x_P, y_P) …	Principal point image coordinates
c …	Principal distance
r_{11} to r_{33} …	Elements of the 3D rotation matrix
(X, Y, Z) …	Object coordinates of reconstructed point
(X_0, Y_0, Z_0) …	Object coordinates of perspective centre
$(\Delta x, \Delta y)$ …	Distortions in image space

References:

[1] _____, *Engineering and Design: Structural Deformation Surveying*, Engineer Manual No. 1110-2-1009, US Army Corps of Engineers, Washington, DC, P. 292, 2002.

[2] K. Kraus, *Photogrammetry, Volume 1: Fundamentals and Standard Processes*, 4th ed., Ferd. Duemmlers Verlag, Bonn, P. 397, 1993.

[3] N.G. Shrive. *Intelligent structural health monitoring: a civil engineering perspective*, IEEE International Conference on Man and Cybernetics, 2005.

[4] A.F. Habib and M.F. Morgan, *Automatic calibration of low-cost digital cameras,* Journal of Optical Engineering, Vol. 42, No. 4, P. 948-955, 2003.

[5] A.F. Habib and M.F. Morgan, *Stability analysis and geometric calibration of off-the-shelf digital cameras,* Photogrammetric Engineering & Remote Sensing, Vol. 71, No. 6, P. 733-741, 2005.

[6] M. Okutomi and T. Kanade, *A Multiple-Baseline Stereo,* IEEE Transactions on Pattern Analysis and Machine Intelligence, Vol. 15, No. 4, P. 353-363, 1993.

[7] C. Harris and M. Stephens. *A combined corner and edge detector*, 4th Alvey Vision Conference, Manchester, UK, 1988.

[8] T. Schenk, *Digital photogrammetry*, Laurelville, Ohio, TerraScience, P. 422, 1999.

[9] F. Ackermann and M. Hahn, *Image pyramids for digital photogrammetry*, in *Digital Photogrammetric Systems*, Ebner H., D. Fritsch, and C. Heipke, Editors, Wichmann Verlag: Karlsruhe, Germany, P. 43-58, 1991.